Observation of enhanced excitation of I_2^{2+} by strong laser fields

G. N. Gibson, R. N. Coffee, and L. Fang
Department of Physics, University of Connecticut, Storrs, Connecticut 06269, USA
(Received 19 September 2005; revised manuscript received 21 November 2005; published 17 February 2006)

Using pump-probe spectroscopy with ultrashort laser pulses, we see an enhancement of the charge-asymmetric dissociation (CAD) channel, $(I_2^{2+})^* \rightarrow I^{2+}+I$, over a narrow range of internuclear separation. The enhancement of the CAD channel appears to come from the excitation of the symmetric ground state dissociation channel ($I^+ + I^+$) for two reasons. First, there is a depletion in the symmetric channel at approximately the same pump-probe delay as the asymmetric enhancement. Second, for a fixed delay, the asymmetric channel increases as a function of probe intensity while the symmetric channel decreases. In addition, we find that the kinetic energy of the extra $I^{2+}+I$ ions decreases for increasing delay. To explain this dependence of the kinetic energy release on delay, we introduce model potential energy curves. Based on these curves, we conclude that the excitation is produced by a resonant three-photon transition within I_2^{2+} rather than by ionization of I_2^+.

DOI: 10.1103/PhysRevA.73.023418 PACS number(s): 33.80.Rv, 32.80.Rm, 42.50.Hz

I. INTRODUCTION

The behavior of atoms and molecules in strong laser fields has been studied for many years [1]. For the most part, both experiment and theory have focused on multiphoton ionization [2], high harmonic generation [3], and rotational [4], or vibrational control [5]. The possibility of direct electronic excitation has received much less attention [6], partly due to the lack of experimental [7,8] and theoretical evidence [9] for electronic excitation in atoms, except for Ref. [10].

In contrast to atoms, the excitation of molecules has been observed in a number of experiments, including photoelectron [11], ion [12], and VUV fluorescence spectroscopy [8,13,14]. Moreover, a recent theory [15] has demonstrated that the nearly degenerate strongly coupled ionic states present in a double-well potential [16] can facilitate high-order multiphoton transitions. An important prediction of this theory is that the excitation rate will be strongly dependent on the internuclear separation, R. In order to test this theory, we performed a pump-probe experiment on I_2 molecules. The pump pulse initiates the dissociation of the molecule. By varying the probe delay, we can measure excitation and ionization rates as a function of R as the molecule comes apart.

In this experiment, we focus on the doubly ionized molecular ion, I_2^{2+}, since it has two distinct dissociation channels: one associated with the electronic ground state of the molecule (1,1), and one associated with the electronically excited ionic states (2,0). [Throughout this paper, (n,m) refers to the $I_2^{(n+m)+} \rightarrow I^{n+}+I^{m+}$ dissociation channel [17].] Moreover, the (2,1) dissociation channel of I_2^{3+} gives a measure of the ionization of the I_2^{2+} channels. Thus, the (1,1), (2,0), and (2,1) signals allow us to measure both excitation and ionization of the I_2^{2+} molecule. We find that all three signals vary as a function of probe delay demonstrating that the probe pulse induces excitation and ionization over distinct ranges of R. There is a minimum in the (2,0) signal corresponding to enhanced ionization over a fairly small range of R [18]. However, we also find a maximum in the (2,0) signal as a function of R that indicates *excitation* of the parent I_2^{2+} molecule by the probe pulse.

This experiment is similar in design to the one performed by Corkum *et al.*, in Ref. [18] to explore enhanced ionization as a function of internuclear separation. However, we improved our temporal resolution compared to Ref. [18] by using 23 fs laser pulses and a pump-probe technique that eliminates interference between the pump and probe pulse near zero time delay. We also use a significantly weaker probe pulse to reduce the effects of ionization. These modifications allow us to observe the R-dependent excitation of I_2^{2+} that otherwise would not be apparent.

By far the biggest impediment to a detailed understanding of our results is a lack of knowledge of the potential energy curves of the various dissociation channels of I_2. This leads to two problems. First, we study excitation and ionization as a function of pump-probe delay, but to convert from delay to internuclear separation, we need to know the potential energy curve on which the molecule is dissociating. Second, when we measure a particular dissociation channel we can determine the kinetic energy release (KER) of the ions and we find that the KER of the (2,0) channel depends on the probe delay. We can use this information to identify the initial charge state of the transition leading to the (2,0) channel, but only if we know the relevant potential energy curves. So, as a simple approximation, we create model potential energy curves as close to Coulomb curves as possible and still be consistent with the measured KER of the different dissociation channels produced by the pump pulse alone. From these curves, we conclude that the enhancement of the (2,0) channel comes from excitation of the (1,1) ground state through a three-photon resonance, rather than ionization from I_2^+ directly into an excited state of I_2^{2+}. Furthermore, the efficiency of this transition is very high, as the probe pulse can increase the (2,0) signal by 20% over the signal from the pump pulse alone.

II. EXPERIMENT

We performed these experiments with a standard Ti:sapphire laser system consisting of a short-pulse oscillator and multipass amplifier [19]. The final output is a laser pulse

with a duration of 23 fs, an energy of 600 μJ, a central wavelength of 800 nm, and a repetition rate of 1 kHz. In these experiments, we generally use a pump energy of 80 μJ focused to a roughly 35 μm diam spot, producing an intensity of about 4×10^{14} W/cm^2. Iodine is leaked effusively into a high vacuum chamber with a base pressure of 10^{-9} torr and the laser induced ions are measured with a standard Wiley-McLaren time-of-flight (TOF) spectrometer [20].

For these experiments, we need both the pump and probe laser pulses to be linearly polarized along the axis of the TOF spectrometer. As the pump and probe pulses also have the same spectrum and direction of propagation, they will interfere near zero time delay. Even a weak probe can strongly modulate the pump pulse intensity when the pulses overlap in time. This generally leads to large fluctuations in the signal, making the data at small time delays unusable. However, two pulses will not interfere and their energies add linearly if they are 90° out of phase, even if their pulse envelopes overlap in time. To impose a 90° phase shift between the pump and probe pulses, we sample a small part of the beam with a pick-off mirror after they are recombined with a beamsplitter. We monitor the sample beam with a photodiode and a single channel analyzer (SCA). We set the SCA to trigger the data acquisition electronics only if the total energy is within a 10% window. While the pulses overlap in time, the only way to trigger the SCA is if they are 90° out of phase. The absolute phase difference between the pump and probe fluctuates sufficiently so that at any particular time delay there are some pulse pairs with the desired phase shift. This may only be a small fraction of the total number of laser shots, which slows down the data acquisition rate near zero time delay. Nevertheless, the resulting data are free of interference effects. Of course, when the pulses are not overlapped in time, their phase difference does not affect the sum of their energies and the SCA only serves to remove energy fluctuations from the laser system.

Three types of experiments were run. First, the pump to probe energy ratio was fixed at 4:1, while the delay was scanned. This yields the excitation and ionization rates as a function of internuclear separation. Second, the delay was fixed and the probe intensity was varied. This reveals the intensity dependence of these processes. Third, we used a weak pump and a strong probe in a ratio of 1:4. This produces strong ionization of the dissociating fragments. While the third experiment masks the enhanced excitation, it allows us to test our model potential energy curves.

III. EXPERIMENTAL RESULTS

Figure 1 shows a typical TOF spectrum of the I^{2+} ions with just the pump pulse. The spectrum consists of characteristic pairs of peaks due to ions initially directed towards and away from the detector. The difference in arrival time between the two peaks is proportional to the initial momentum of the ions. The peaks are labeled with the charge of the two dissociating ions, as mentioned above. All of the dissociation channels have been previously identified through correlations [12]. The center peak at a TOF for zero kinetic energy comes from the ionization of iodine atoms that are

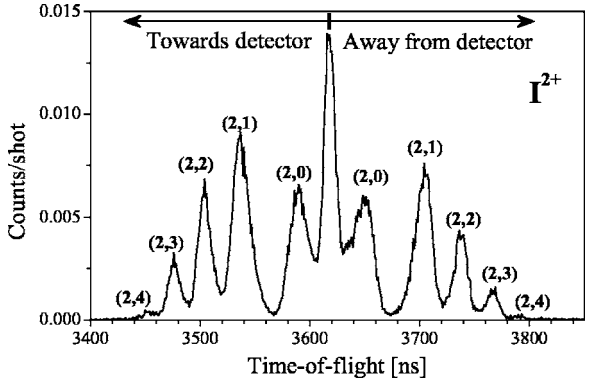

FIG. 1. TOF spectrum for the I^{2+} ions. The label (n,m) refers to the $I_2^{(n+m)+}\rightarrow I^{n+}+I^{m+}$ dissociation channel.

present because amplified spontaneous emission from the laser system produces low energy dissociation of I_2. This has previously been shown to not affect the molecular peaks [21].

Figure 2 shows the same I^{2+} TOF region, with both the pump and probe pulse, as a function of time delay between the pulses. The ion TOF now runs along the vertical axis and the pump-probe delay along the horizontal axis. Each peak in Fig. 1 produces a horizontal "track" in Fig. 2 and the channels that we are concerned with, (2,0) and (2,1), are labeled. It is quite clear that the (2,0) signal is strongly modified by the probe pulse: at a delay of about 50 fs (a), there is an increase in the (2,0) signal, while at 125 fs delay (b), there is a decrease, compared to the signal at long time delay. The data are smooth down to zero time delay because our pump-probe technique avoids fluctuations due to interference. Similar data were collected for the I^{1+} TOF spectrum.

Although the two-dimensional (2D) plot shows the overall behavior, more quantitative information is gained by plotting just the magnitudes of the (1,0), (1,1), (2,0), and (2,1) signals as a function of the pump-probe delay, shown in Fig. 3. In this figure we see the reduction of the (2,0) channel

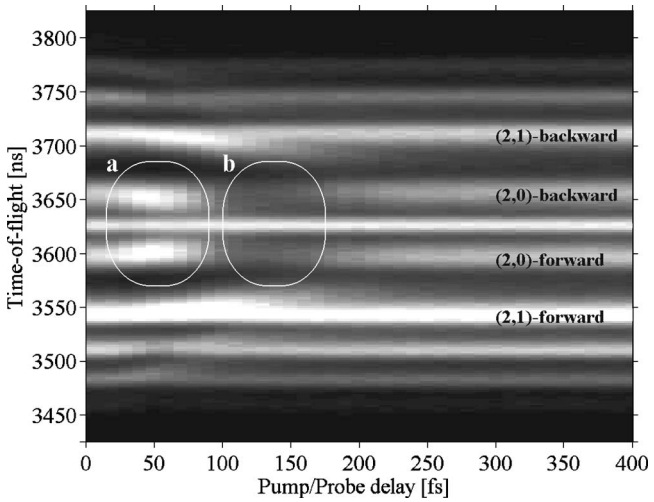

FIG. 2. TOF spectrum for the I^{2+} ions as a function of pump-probe delay. The delay was scanned in 10 fs steps. (a) is the region of excitation; (b) is the region of ionization.

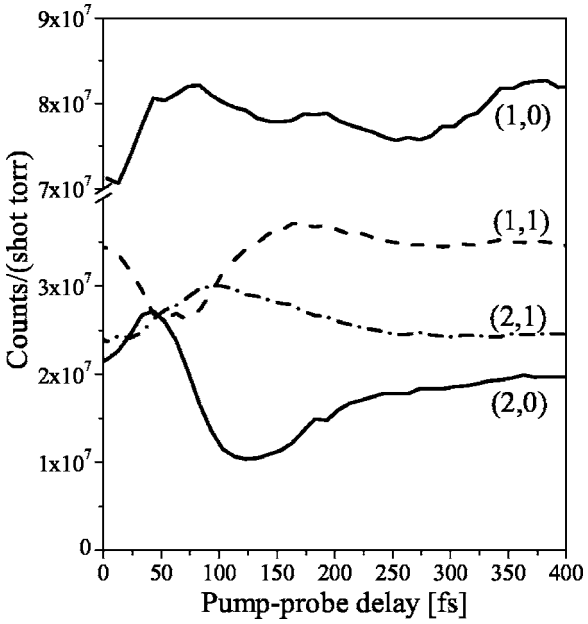

FIG. 3. Individual dissociation channels as a function of pump-probe delay. The pump/probe ratio is 4:1 and the peak pump intensity is 4×10^{14} W/cm^2.

around delays of 100–150 fs due to enhanced ionization of (2,0) to (2,1) [18]. At the same time, there is an increase in the (2,1) channel, as would be expected for ionization of (2,0) to (2,1). However, there is also a pronounced enhancement of (2,0) at time delays near 50 fs. Coincident with this is a decrease in (1,1) suggesting that the (2,0) signal increases at the expense of the (1,1) signal. Such anticorrelated signals show that the probe pulse transfers population from the (1,1) channel to the (2,0) channel when it follows the pump pulse by 50 fs. To further test this anticorrelation we kept the probe delay fixed at 64 fs, at the minimum of the (1,1) signal, and varied the probe intensity. The results are shown in Fig. 4 and, again, demonstrate that the change in the (1,1) signal is just the opposite of the (2,0) signal. In both Figs. 3 and 4, the maximum increase in the (2,0) signal strength is around 20% of the signal with the pump pulse

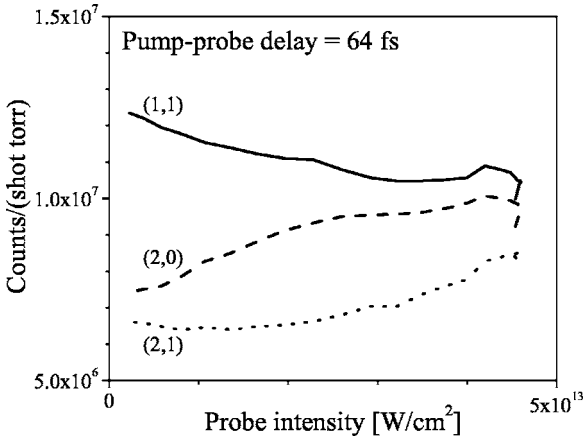

FIG. 4. Individual dissociation channels as a function of probe intensity. Pump intensity is 1.7×10^{14} W/cm^2.

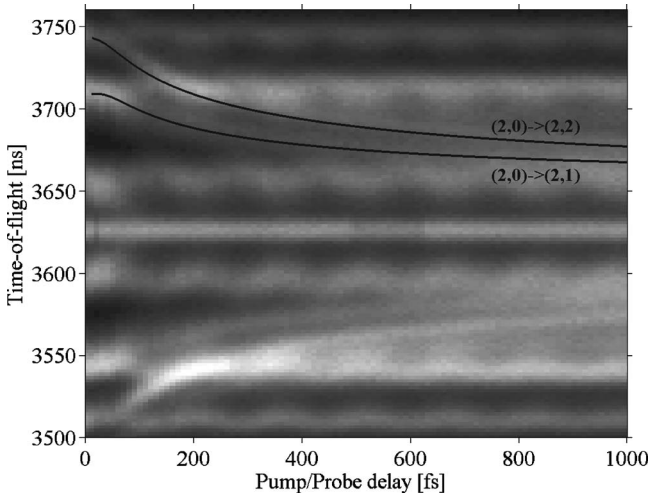

FIG. 5. Pump-probe data with a strong probe pulse to saturate the ionization of the dissociation channels. The black lines show the KER for ions starting on the (2,0) potential energy curve and ionizing to the (2,1) or (2,2) curves, as a function of delay. Note that the TOF spectrum is symmetric around the zero kinetic energy point, at 3625 ns. The early TOF region is shown without the predicted curves overlaid, so as to show the ionization tracks more clearly.

alone, indicating a rather high efficiency of the population transfer.

Finally, to obtain some information about the potential energy curves of the different charge states of I_2, we ran the pump-probe experiment with the opposite ratio of pump to probe energy, 1:4, shown in Fig. 5. This produces more complete ionization as the molecules dissociate and forms curved tracks in the 2D pump-probe plots because the KER in a two step ionization process will depend on the delay between the pulses. Both curved tracks in Fig. 5 start with ionization to the (2,0) channel by the weak pump pulse. If the strong probe pulse immediately ionizes the dissociating molecule to the (2,1) potential energy curve, the ions will experience the full Coulomb repulsion of this channel. However, if the strong probe is delayed substantially, then the ionic fragments are far from each other and will gain little additional energy. Thus, for long delay, these (2,1) ions will have a KER equal to the single pulse (2,0) channel. In this way, the KER of any dissociation channel formed in two steps will depend on the time delay between the two pulses. Moreover, this dependence is determined by the potential energy curves of the different molecular charge states. While we measure this delay dependent KER, these data cannot be unambiguously inverted to get individual potential energy curves. However they can provide a consistency check on the model curves. In fact, the ionization tracks predicted from our model potential energy curves, discussed below and shown in Fig. 5, agree well with the data. The strong periodic modulation in these data occurs when the pump pulse produces vibrational excitation in the neutral molecule without ionization. It only occurs for a weak pump and strong probe pulse and no such modulation is seen in our main data set, Fig. 2.

IV. POTENTIAL ENERGY CURVES

Before discussing the dynamics of the dissociating I_2 molecules, we need to address the potential energy curves for the different charge states for the molecule. Many groups have used simple Coulomb curves to interpret the KER from the strong field ionization of diatomic molecules [22,23]. Since the measured kinetic energies consistently fall short of the values expected from a Coulomb potential at the equilibrium internuclear separation of the neutral molecule, R_e, it was assumed that the molecules first expand to a larger separation during the laser pulse before being ionized to higher charge states [22]. Then the measured KER was used to determine the internuclear separation at which the ionization occurred by simply projecting the kinetic energy onto a Coulomb potential energy curve. At the same time, it was also realized that the potential energy curves have a significant binding term, even for very high molecular charge states. This leads to large deviations from a pure Coulomb potential at small values of R [24,25]. If the molecule expands during the laser pulse and the potential energy curves are unknown, it is difficult to gain much insight from the KER's. However, attempts have been made to take both effects into account using various approximations [20,26,27].

In the limit of a heavy molecule and a short laser pulse, molecular expansion during the laser pulse is minimal, simplifying the analysis of the KER's. This is the reason we chose to study iodine with 23 fs laser pulses. Given the potential energy curves defined below in Eqs. (1)–(3), we estimate the increase in the internuclear separation during the laser pulse will be at most 0.2 Å beyond the equilibrium value of 2.66 Å. These curves then provide the connection between the pump-probe delay and the internuclear separation. One immediate consequence of these curves is that, although counterintuitive, the charge states that *initially* move the fastest are likely to be the (1,0) and (2,0) channels. This is because we are ionizing to the steep inner wall of the potential energy curve where the dissociating ions feel a strong acceleration. Ions on potential curves with a Coulomb repulsion, like the (1,1) channel, ultimately gain a greater kinetic energy, but initially do not accelerate as fast as the (1,0) and (2,0) channels because of the long range nature of the Coulomb interaction. So, for example, in the region of interest for excitation and ionization dynamics, where $R_e \leqslant R \leqslant 2R_e$, the (1,0) and (2,0) dissociation fragments move faster than the (1,1) fragments.

There are actually a fair number of calculations of the low lying states of I_2^+ [28,29]. Many of these states are bound and produce the I_2^+ ion peak in the TOF spectrum. However, there are also low lying curves, which if populated at R_e would dissociate with the observed kinetic energy for this channel. Thus, we have simply used a Morse potential with values similar to the calculated curves which also yield the measured KER of the (1,0) channel (all of the following potential energy curves are in atomic units, a.u.):

$$U_{1,0}(R) = D_e\left[1 - e^{-(R-R_o)/d}\right]^2, \tag{1}$$

where $D_e=0.037$ a.u., $R_o=7$ a.u., and $d=2.38$.

For $I^+ + I^+$, as mentioned above, the Coulomb curve would predict too high a KER for ionization at R_e. While this high KER can be reduced in a number of ways, the motion along the curve is not too sensitive to the details of the curve as the dissociation is dominated by the Coulomb repulsion. Following the qualitative arguments of Ref. [25], we simply assume a slight screening of the Coulomb curve and let

$$U_{1,1}(R) = a_{1,1}/R, \tag{2}$$

where $a_{1,1}=0.8$. Here, $a_{1,1}$ is chosen to produce the measured KER for the (1,1) channel.

The I_2^{2+} curve leading to the (2,0) dissociation channel is a little more complicated. It has been assumed that the curve is quite flat and the (2,0) dissociation will be at a constant velocity [18]. While this is true for large R, the details of the curve at small R are quite important because a flat curve produces no acceleration. There will clearly be a strong polarization attraction for intermediate values of R as well as a repulsive inner wall. The polarizability of neutral atomic iodine is about $\alpha=5$ Å^3 [30–32]. In the presence of an I^{2+} ion this will produce an attractive $1/R^4$ potential. For the short range repulsion, we simply add a $1/R^5$ term with a coefficient that reproduces the measured KER. The resulting curve is

$$U_{2,0}(R) = -\alpha(2/R^2)^2 + \beta/R^5 + D_{2,0}, \tag{3}$$

where $\alpha=34$ a.u.^{3}, $\beta=800$ a.u.^{4}, and $D_{2,0}=0.32$ a.u. $D_{2,0}$ is the difference between the (2,0) and (1,1) asymptotic limits and is equal to the difference in the ionization potentials of I and I^+ [33]. Finally, for the (2,1) and (2,2) curves, we use Coulomb curves with a screening of $\alpha_{2,1}=\alpha_{2,2}=0.76$.

Once these curves are defined, it is a simple matter to integrate the motion along the curves and predict the KER of a molecular ion in a double pulse experiment. The pump pulse ionizes the neutral molecule to the initial charge state, which then begins to dissociate. From the potential energy curve, we know the internuclear separation as a function of time during the dissociation. The probe pulse then ionizes the dissociating molecule to a higher charge state. This yields the KER release as a function of pump-probe delay that we can directly compare to the data in Fig. 5. In this plot, the changing KER as a function of delay will show up as a curved track. The most prominent ionization tracks are (2,0) $\rightarrow$ (2,1) and (2,0) $\rightarrow$ (2,2) with the predicted dependence shown as solid lines. The fact that the predicted tracks fit the data well lends support to our hypothetical potential curves [Eqs. (1)–(3) above].

V. DISCUSSION

Our main observation is that over a small range of pump-probe delay there is an increase in the (2,0) asymmetric dissociation signal. This occurs before the better understood region of enhanced ionization. The extra (2,0) ions can only come from I_2, I_2^+, or I_2^{2+} molecules. However, we can rule out bound or metastable states of these species, since these would either show no delay dependence or a periodic dependence due to possible vibrational excitation. Since the enhancement of the (2,0) signal has a non periodic dependence

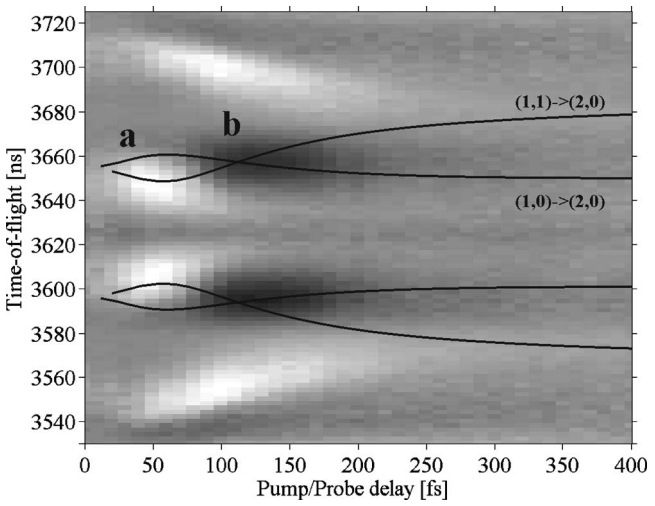

FIG. 6. Pump-probe data from Fig. 2 with the signal from the large delay subtracted. The black lines show the predicted KER for the two processes (1,0)→(2,0) and (1,1)→(2,0). (a) region of excitation to (2,0), (b) region of ionization of (2,0). Note the expanded vertical scale.

on delay, the precursor to the (2,0) signal can only be the (1,0) or (1,1) dissociation channels. From the delay dependences shown in Fig. 3, we conclude that the increase in (2,0) comes from a depletion of the (1,1) signal rather than the (1,0) signal, as the (1,0) signal stays relatively constant

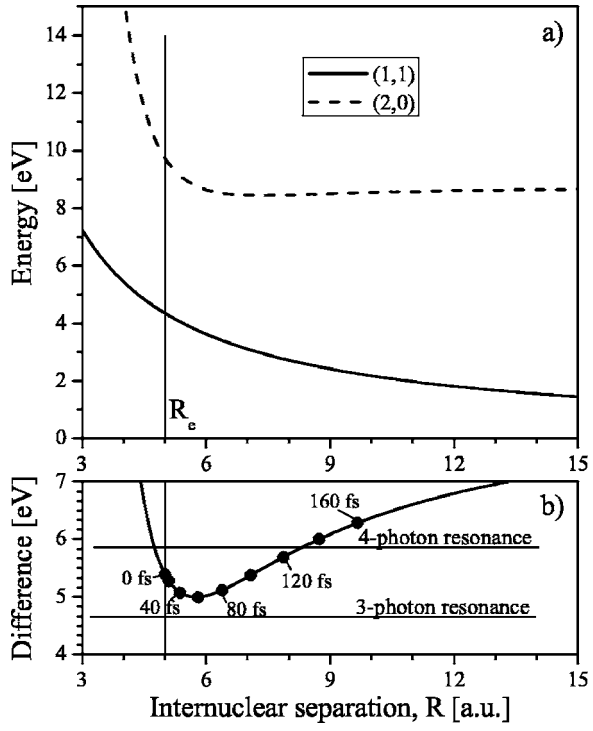

FIG. 7. (a) Potential energy curves of the (1,1) and (2,0) dissociation channels. (b) Difference between the (1,1) and (2,0) curves along with the energies of a three-photon and four-photon resonance with 800 nm light. The dots in the lower graph show the internuclear separation at 20 fs intervals, if the molecule dissociates on the (1,1) potential energy curve.

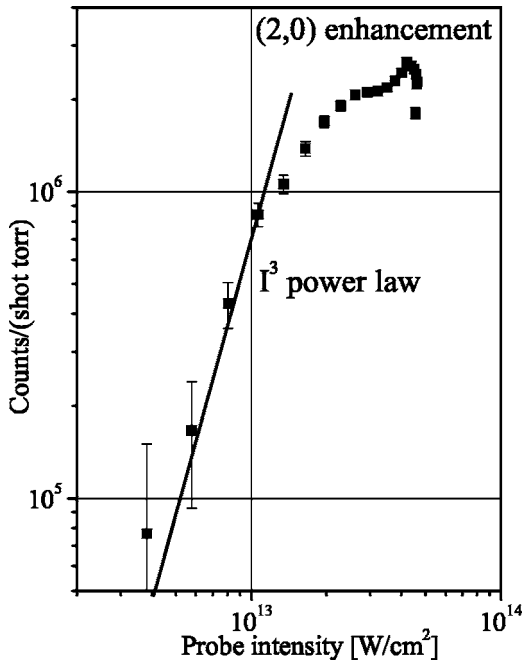

FIG. 8. Log-log plot of the enhancement of the (2,0) signal from Fig. 4 as a function of probe intensity. The error bars include both the statistical uncertainty in each data point and the systematic error from the background subtraction.

after about 25 fs and certainly does not show a dip where the (2,0) signal peaks. As mentioned above, Fig. 4 strengthens this notion by showing that the (1,1) and (2,0) signals are also anticorrelated as a function of probe intensity. These observations suggest that the probe pulse is transferring the population from (1,1) to (2,0). The (1,1) depletion does not perfectly mirror the (2,0) enhancement because the ionization of the (2,0) channel begins to compete at larger values of R. This does not affect the (1,1) depletion but does reduce the (2,0) enhancement at later time delays.

So far, we have focused on the amplitudes of the various dissociation channels. However, in Fig. 2, it is clear that the KER of the (2,0) channel decreases as a function of delay over the range where there is an enhancement in the amplitude of this signal. As discussed above, the KER of any channel depends on the potential energy curves. Therefore, excitation from one channel to another at different internuclear separations should change the KER.

In order to focus on just the extra (2,0) ions, we have taken the data in Fig. 2 and subtracted the average TOF spectrum between 900 and 1000 fs, where the signals are no longer changing as a function of time delay. The data with this background subtracted are shown in Fig. 6. This emphasizes both the enhancement in the (2,0) signal at around 50 fs, (a) and the depletion around 140 fs, (b). It also brings out the changing KER release as a function of delay.

Using the potential energy curves discussed above, we can predict the KER for the two processes (1, 0)→(2, 0) and (1, 1)→(2, 0). While the potential energy curves are rather speculative, they give quite different predictions. Based on the initial slope of the KER versus delay, the data clearly favor (1,1)→(2,0). From this we again conclude that we are,

in fact, observing a direct excitation from the (1,1) dissociating state of I_2^{2+} to the (2,0) excited ionic state of the molecule.

The last consideration is the mechanism for this excitation. Figure 7 shows the (1,1) and (2,0) potential energy curves, from Eqs. (2) and (3), as well as the difference between them. The model potential energy curves predict a near three-photon resonance which would be reached at about 50 fs by molecules on the (1,1) dissociation curve. Moreover, the difference between the two curves is flat in this region, helping the excitation rate. Unfortunately, this is not a definitive interpretation of the data, since the curves are too speculative. Nevertheless, it has recently been predicted that such multiphoton transitions between the covalent ground state and the excited ionic states should be quite strong in ionized diatomic molecules [15]. If the excitation is indeed a three-photon resonance, then the enhancement of the (2,0) signal should increase as the cube of the probe intensity. Measuring an accurate intensity dependence is difficult in the presence of a large background. This is the case, here, as the pump pulse produces its own (2,0) signal. Nevertheless, we can take the data in Fig. 4 and subtract the signal strength of the data point at the lowest intensity. If we plot the rest of the data for the (2,0) signal on a log-log plot, Fig. 8, we do find a cubic intensity dependence. At higher intensities, ionization begins to set in, leading to a saturation of the signal. Again, subtracting a background before fitting a power law to the data adds a level of uncertainty to the result, but the data are at least consistent with a three-photon process.

VI. CONCLUSIONS

In conclusion, we have experimentally demonstrated excitation from the symmetric (1,1) dissociating state of I_2^{2+} to an ionic state, approximately 5 eV higher in energy. This appears to correspond to a resonant 3-photon transition and the efficiency of the transfer can be as high as 20%. The possibility of such a strong high-order multiphoton transition has recently been predicted for generic double-well potentials and thus should occur in all dissociating homonuclear diatomic molecules.

ACKNOWLEDGMENT

We would like to acknowledge support from the NSF under Grant No. NSF-PHYS-0244658.

[1] *Atoms in Intense Laser Fields*, edited by M. Gavrila (Academic Press, Boston, 1992).
[2] See, for example, B. Walker, B. Sheehy, L. F. DiMauro, P. Agostini, K. J. Schafer, and K. C. Kulander, Phys. Rev. Lett. **73**, 1227 (1994).
[3] See, for example, M. Bellini, C. Lynga, A. Tozzi, M. B. Gaarde, T. W. Hansch, A. L'Huillier, and C.-G. Wahlstrom, Phys. Rev. Lett. **81**, 297 (1998).
[4] K. F. Lee, I. V. Litvinyuk, P. W. Dooley, M. Spanner, D. M. Villeneuve, and P. B. Corkum, J. Phys. B **37**, L43 (2004).
[5] R. A. Bartels, T. C. Weinacht, S. R. Leone, H. C. Kapteyn, and M. M. Murnane, Phys. Rev. Lett. **88**, 033001 (2002).
[6] C. K. Rhodes, Science **229**, 1345 (1985).
[7] P. H. Y. Lee, D. E. Casperson, and G. T. Schappert, Phys. Rev. A **40**, 1363 (1989).
[8] R. N. Coffee and G. N. Gibson, Phys. Rev. A **69**, 053407 (2004).
[9] R. E. Duvall, E. J. Valeo, and C. R. Oberman, Phys. Rev. A **37**, 4685 (1988).
[10] M. P. Hertlein, P. H. Bucksbaum, and H. G. Muller, J. Phys. B **30**, L197 (1997).
[11] G. N. Gibson, R. R. Freeman, and T. J. McIlrath, Phys. Rev. Lett. **67**, 1230 (1991).
[12] D. T. Strickland, Y. Beaudoin, P. Dietrich, and P. B. Corkum, Phys. Rev. Lett. **68**, 2755 (1992); G. N. Gibson, M. Li, C. Guo, and J. P. Nibarger, Phys. Rev. A **58**, 4723 (1998).
[13] G. Gibson, T. S. Luk, A. McPherson, K. Boyer, and C. K. Rhodes, Phys. Rev. A **40**, 2378 (1989).
[14] R. N. Coffee and G. N. Gibson, Phys. Rev. A **72**, 011401(R) (2005).
[15] G. N. Gibson, Phys. Rev. Lett. **89**, 263001 (2002); G. N. Gibson, Phys. Rev. A **67**, 043401 (2003).
[16] R. S. Mulliken, J. Chem. Phys. **7**, 20 (1939).
[17] G. N. Gibson, M. Li, C. Guo, and J. P. Nibarger, Phys. Rev. A **58**, 4723 (1998).
[18] E. Constant, H. Stapelfeldt, and P. B. Corkum, Phys. Rev. Lett. **76**, 4140 (1996).
[19] M. Li and G. N. Gibson, J. Opt. Soc. Am. B **15**, 2404 (1998).
[20] J. P. Nibarger, S. V. Menon, and G. N. Gibson, Phys. Rev. A **63**, 053406 (2001).
[21] J. P. Nibarger, M. Li, S. Menon, and G. N. Gibson, Phys. Rev. Lett. **83**, 4975 (1999).
[22] K. Codling, L. J. Frasinski, and P. A. Hatherly, J. Phys. B **22**, L321 (1989).
[23] Ph. Hering and C. Cornaggia, Phys. Rev. A **59**, 2836 (1999).
[24] A. D. Bandrauk, D. G. Musaev, and K. Morokuma, Phys. Rev. A **59**, 4309 (1999).
[25] J. S. Wright, G. A. DiLabio, D. R. Matusek, P. B. Corkum, M. Yu. Ivanov, Ch. Ellert, R. J. Buenker, A. B. Alekseyev, and G. Hirsch, Phys. Rev. A **59**, 4512 (1999).
[26] C. Cornaggia and L. Quaglia, Phys. Rev. A **63**, 030702(R) (2001).
[27] S. V. Menon, J. P. Nibarger, and G. N. Gibson, J. Phys. B **35**, 2961 (2002).
[28] J. Li, and K. Balasubramanian, J. Mol. Spectrosc. **138**, 162 (1989).
[29] W. A. de Jong, L. Visscher, and W. C. Nieuwpoort, J. Chem. Phys. **107**, 9046 (1997).
[30] K. Drühl, J. Chem. Phys. **75**, 5579 (1981).
[31] J. Vigue, M. Saute, and M. Aubert-Frécon, J. Chem. Phys. **78**, 4544 (1983).
[32] http://nautilus.fis.uc.pt/st2.5/
[33] *CRC Handbook of Chemistry and Physics*, edited by D. R. Lide (CRC Press, Boca Raton, 1992), pp. 10–213.